Single mutations convert an outward K^+ channel into an inward K^+ channel

Legong Li*†, Kun Liu†, Yong Hu*, Dongping Li‡, and Sheng Luan†§

*College of Life Sciences, Capital Normal University, Beijing 100037, China; †Department of Plant and Microbial Biology, University of California, Berkeley, CA 94720; and ‡College of Life Sciences, Hunan Normal University, Changsha 410006, China

Communicated by Bob B. Buchanan, University of California, Berkeley, CA, December 29, 2007 (received for review October 1, 2007)

Shaker-type K^+ channels in plants display distinct voltage-sensing properties despite sharing sequence and structural similarity. For example, an *Arabidopsis* K^+ channel (SKOR) and a tomato K^+ channel (LKT1) share high amino acid sequence similarity and identical domain structures; however, SKOR conducts outward K^+ current and is activated by positive membrane potentials (depolarization), whereas LKT1 conducts inward current and is activated by negative membrane potentials (hyperpolarization). The structural basis for the "opposite" voltage-sensing properties of SKOR and LKT1 remains unknown. Using a screening procedure combined with random mutagenesis, we identified in the SKOR channel single amino acid mutations that converted an outward-conducting channel into an inward-conducting channel. Further domain-swapping and random mutagenesis produced similar results, suggesting functional interactions between several regions of SKOR protein that lead to specific voltage-sensing properties. Dramatic changes in rectifying properties can be caused by single amino acid mutations, providing evidence that the inward and outward channels in the Shaker family from plants may derive from the same ancestor.

Arabidopsis | ion channels | voltage-gating | DNA shuffling | mutagenesis

The largest group of voltage-gated K^+ channels is the Shaker family, which was named after the first cloned K^+ channel from *Drosophila* (1, 2). Most of the channels in the Shaker family from animals are activated upon membrane depolarization and conduct outward currents. These channels consist of four subunits, each of which contains six transmembrane helices, referred to as S1–S6 (3). Regarding the structural basis of voltage sensitivity, a transmembrane helix S4 harbors multiple positively charged amino acids and serves as a voltage sensor. The region from S5 to S6 constitutes the functional pore of the channel, with a highly conserved signature motif (GYGD) forming a selection filter for K^+ specificity (4, 5). The gate of the channel appears to lie in S6 helices that form a reverse teepee-like structure, limiting the ionic flow across the pore (6). Voltage-gated K^+ channels switch between conducting and nonconducting states as a result of conformational changes in the voltage-sensing domains (7). This gating process is triggered by a cluster of positively charged residues on S4, driving this domain into a "down state" at negative voltages and an "up state" at positive voltages (8). The least understood property of the voltage-gated K^+ channels is how the voltage sensor and the gate are coupled to operate the voltage-dependent opening and closing processes. More intriguing is the fact that different members in the Shaker family may be operated by very different voltage ranges and conduct either outward or inward current, as is the case for Shaker-type channels in plants (9, 10).

Although most Shaker-type channels in animal systems are activated by depolarization and conduct outward K^+ currents, the first group of Shaker-type channels identified in plants, including KAT1 and AKT1, are, surprisingly, activated by hyperpolarization and conduct inward currents (11–13). Later, two outward K^+ channels—SKOR and GORK—with a structure very similar to that of the inward channels, were identified in plants (14, 15). The outward and inward channels not only resemble each other in domain structure (each subunit having S1–S6 organization), but they are also highly similar at the level of amino acid sequence. It is puzzling how channel proteins with such high homology are activated by entirely different membrane voltages (depolarization vs. hyperpolarization) and conduct opposite currents. Associated with this puzzle is the question of how these channels have evolved from one to another, because they appear to come from the same ancestor, based on their similar protein sequences. Here we report a high-throughput screening procedure that enabled us to identify single amino acid mutations in an outward K^+ channel that transformed the channel into an inward rectifier, suggesting that the high similarity of two subfamilies of Shaker channels in plants may have evolved from the same ancestor and that the structural basis for opposite rectification may lie in the variations of single amino acid residues.

CELL BIOLOGY

Results and Discussion

Comparing the Sequences and Voltage-Sensing Properties of Inward and Outward Channels in Plants. We compared the sequences of outward channel SKOR and inward channel LKT1 and found a striking similarity between the two (Fig. 1*A*). These two channel proteins share >35% identity and 67% similarity in the amino acid sequences throughout the entire protein length. The identical matches appear to be widely distributed, with the most similar areas found in the transmembrane S1–S6 domains. Despite the similarity in sequence and domain structures, these two channels show very different kinetics in their voltage-dependent activation. Although SKOR was activated by membrane depolarization, LKT1 responded only to membrane hyperpolarization (Fig. 1*B*). On the basis of the domain and sequence information, we speculated that both depolarization- and hyperpolarization-activated channels may have evolved from the same ancestor and that the structural basis for opposite rectification could be subtle and may lie in variations of single amino acid residues.

A Screening Strategy for Mutants with Altered Functionality of SKOR. Based on the considerations described above, we developed a strategy for identifying the structural determinants of rectification in K^+ channel proteins. We chose to use SKOR as a model channel, to identify amino acid residues that are important for its rectification property. As shown in Fig. 1*C*, a random mutagenesis procedure (error-prone PCR combined with DNA shuffling, as described in refs. 16 and 17) was used to incorporate mutations into the S1–S6 transmembrane domains of SKOR

Author contributions: L.L., K.L., and S.L. designed research; L.L. and K.L. performed research; Y.H. contributed new reagents/analytic tools; L.L., K.L., D.L., and S.L. analyzed data; and L.L., K.L., Y.H., D.L., and S.L. wrote the paper.

The authors declare no conflict of interest.

§To whom correspondence should be addressed. E-mail: sluan@nature.berkeley.edu.

This article contains supporting information online at www.pnas.org/cgi/content/full/0712349105/DC1.

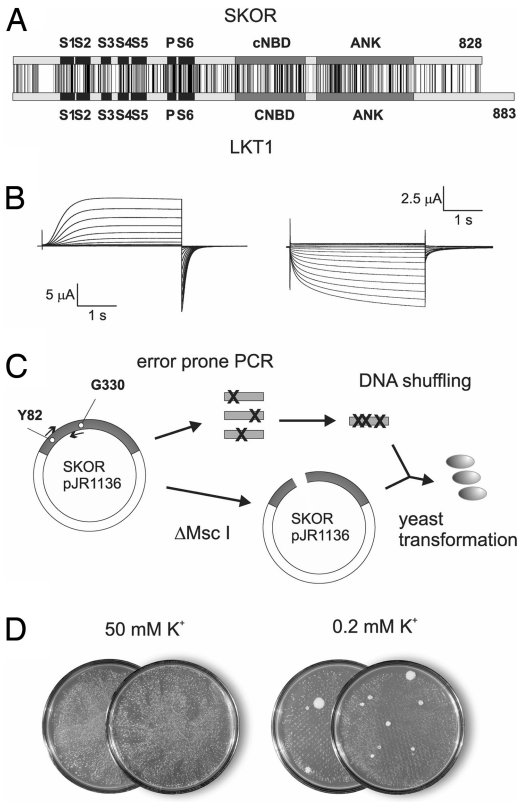

Fig. 1. Functional SKOR mutants selected by random mutagenesis and yeast complementation. (*A*) Diagram showing high homology between SKOR and LKT1. Different domains in both channels are indicated by open and filled bars, including S1–S6 transmembrane regions, cyclic nucleotide-binding domain (cNBD), and Ankyrin repeat domain (ANK). (*B*) Whole-cell currents recorded from oocytes expressing SKOR (*Left*) and LKT1 (*Right*). A TEVC configuration was used with changing test voltages from −150 to +120 mV in 10-mV increments. The holding potential was −40 mV. (*C*) Protocol for screening randomly mutated SKOR channels in yeast mutant CY162. (*D*) Yeast growth on low-K^+ concentration medium (0.2 mM K^+) as an indication of SKOR mutants with K-uptake capability.

protein, with the hope that some mutations would significantly alter the rectification properties of the SKOR channel. The randomly mutagenized SKOR sequences in the pJR1136 vector (18) were transformed into a yeast mutant, CY162, that did not grow on the medium containing <1 mM K^+ (18). Cells from the surviving colonies were replated to select transformants capable of growing on low-K^+ medium. With <0.2 mM K^+, CY162 transformed with the wild-type SKOR channel construct did not survive. Some colonies transformed by the mutagenized SKOR sequences were able to grow under the low-K^+ conditions and might contain SKOR mutant channels with K-uptake capacity. These colonies were selected for further study (Fig. 1*D*). The plasmids were recovered from the colonies, amplified in *Escherichia coli*, and retransformed into yeast mutant CY162. This procedure confirmed that yeast mutant complementation was the result of transformation by SKOR mutants. Independent SKOR mutants were sequenced to determine the sequence modifications responsible for the functional changes in the SKOR channel.

Subtle Amino Acid Changes Convert SKOR into an Inward Rectifier. The capability of SKOR mutants to complement the CY162 mutant under a low-K^+ condition suggested that the SKOR mutants were significantly altered in their channel properties. To examine the kinetic modifications caused by specific mutations in the SKOR protein, the SKOR mutants were studied by electrophysiological procedures using the *Xenopus* oocyte expression system, as described in ref. 19. The channel properties of the SKOR mutants were studied in comparison with wild-type SKOR. In the cases where multiple amino acid residues were altered in one mutant, site-directed mutagenesis was used to determine which amino acid was responsible for the phenotype of the channel mutant.

We focused on one SKOR mutant with two amino acid mutations (D312N and L271P) that supported yeast growth in the same manner as KAT1 (Fig. 2*A*), a typical inward K^+ channel in *Arabidopsis* (11). We recorded whole-cell currents of *Xenopus* oocytes expressing this SKOR mutant, with clamp potentials ranging from +120 to −200 mV. Interestingly, this SKOR mutant (D312N and L271P) was activated by membrane hyperpolarization and conducted inward current, in stark contrast to the wild-type SKOR that was activated by membrane depolarization and conducted only outward current (Fig. 2*B*). Fig. 2*C* shows that the rectifying component of the current had activation kinetics similar to typical inward-rectifying channels, including members of the KAT and AKT subfamilies. From −30 to +120 mV, the mutant channel was fully closed. The channel began to conduct inward currents as the membrane voltage was changed from −30 to −200 mV. Such activation kinetics are exactly opposite to those of wild-type SKOR, which was activated by more positive membrane potentials (−30 to +120 mV). A single-channel recording showed that the mutant channel opened more frequently when the membrane was hyperpolarized (Fig. 2 *D* and *E*), and its activity was nearly undetectable under depolarization conditions, which is consistent with the results from a whole-cell recording.

To further dissect the contribution of the two amino acid changes, we generated site-directed mutations in the wild-type SKOR, including a single mutation at either L271 or D312. We changed L271 to P, V, G, N, K, and D, which represent amino acids with different chemical properties, including side-chain length, charge, and hydrophobicity. Among these single mutants, N, K, and D replacements rendered the channel inactive. The P, V, and G replacements produced functional channels that, like the wild-type SKOR, displayed outward current with delayed activation (Fig. 3*A*). Detailed analysis of the activation kinetics revealed significant change in L271P, namely, the *G–V* curve shifted to the left side significantly, indicating that this channel was facilitated to the open state at more hyperpolarized potential, compared with the wild-type SKOR (Fig. 3*B*). L271G also shifted the *G–V* curve to the more hyperpolarized side, but to a lesser extent.

The D312 position appeared to be less flexible. The only functional channel produced was by a D-to-N replacement among the modifications of D to A, E, L, N, or K. The single mutation D312N rendered the channel voltage-independent (Fig. 3*C*). Upon voltage application in the range of −200 to +120 mV, the currents appeared instantaneously without voltage-dependent activation. This result, which is consistent with previous reports (20, 21), indicates that, in the D312N/L271P double mutant, D312N contributed more to the change in voltage-dependence, and L271P played a role in inward rectification (Fig. 2*B*). In other words, these two positions may interact to control the voltage-sensing property of the SKOR channel cooperatively. To explore this relationship further, we combined D312N with different mutations at the L271 (L to V, G, N, K, and D, respectively). To our surprise, several nonfunctional single mutants (L271N, L271K, and L271D) were rescued by the D312N mutation (Fig. 3*C*). Moreover, the combination of D312N and L271 mutations, like the D312N/L271P double mutant, further modified the channel kinetics found with the D312N single mutant (Fig. 2*B*), supporting the idea that these two positions may functionally interact with each other in

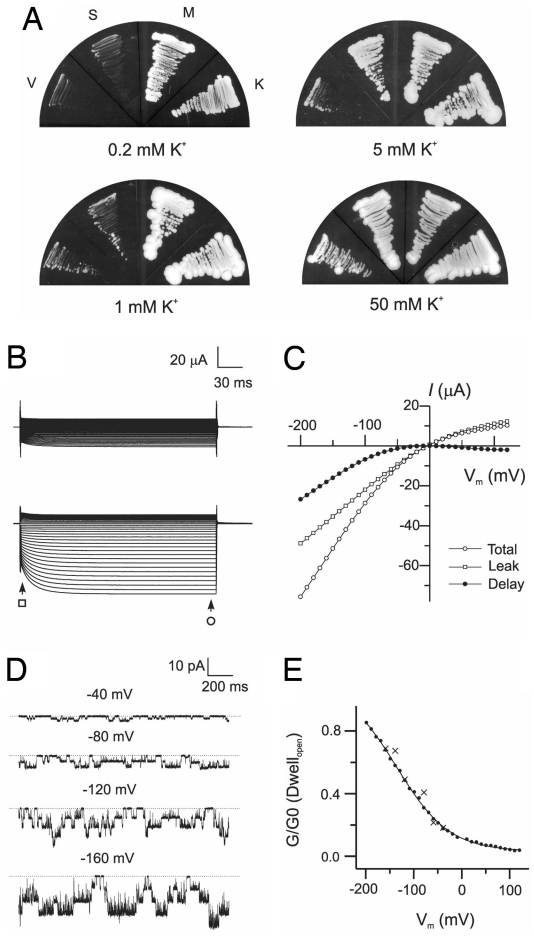

Fig. 2. Two amino acid mutations (D312N/L271P) convert SKOR into an inward rectifier. (*A*) Growth of CY162 yeast mutant transformed with vector only (V), wild-type SKOR (S), mutant D312N/L271P (M), or KAT1 (K). Growth was monitored under different K^+ concentrations. (*B*) Whole-cell currents recorded from oocytes expressing SKOR double mutant (D312N/L271P) by the TEVC configuration, with changing test voltages from −200 to +120 mV in 10-mV increments. The bath solutions contained 10 mM (*Upper*) and 100 mM (*Lower*) KCl. The scale bars are for both traces. (*C*) Current–voltage (*I–V*) curves based on data from *B* with 100 mM KCl in each voltage-clamp episode ($t = 240$ ms; $n = 5$ for each group). Different components of currents were calculated at a different scanning time, as indicated by open circles (total currents at 230 ms), open squares (leak currents at 10 ms), and filled circles (delayed inward currents; difference between total currents and leak currents). (*D*) Selected single-channel current traces from a representative inside-out patch perfused with 2 mM K^+ in the bath solution. The pipette solution contained 100 mM K^+. The voltage protocol is described above the current traces. The bath solution contained 100 μg/ml nystatin for permeability. (*E*) Voltage-dependence of SKOR double mutant (D312N/L271P). Single-channel activation based on *D* at membrane voltages from −200 to +120 with 10-mV increments. The single-channel conductance (γ) was calculated by linear approximation as $\gamma = i/(V - V_{rev})$, where i is the single-channel unitary current and V is the membrane potential. In the patches with multichannel activities, the unitary current was measured from the first current step from the basal level. The number of active channels was derived from the number of current steps in the most active condition. The average conductance of multichannel (G) was normalized to the largest conductance (G_0) to acquire the relative conductance (G/G_0) vs. the membrane potentials. The smooth trace is the best-fitting curve of relative conductance derived from Boltzmann's law $P_o = P_{omax}/(1 + e^{-z_g \cdot F \cdot (V - V_{1/2})/RT})$ and equation $1 = G \cdot (V - V_{rev}) = P_o \cdot \gamma \cdot N \cdot (V - V_{rev})$, as described in ref. 26.

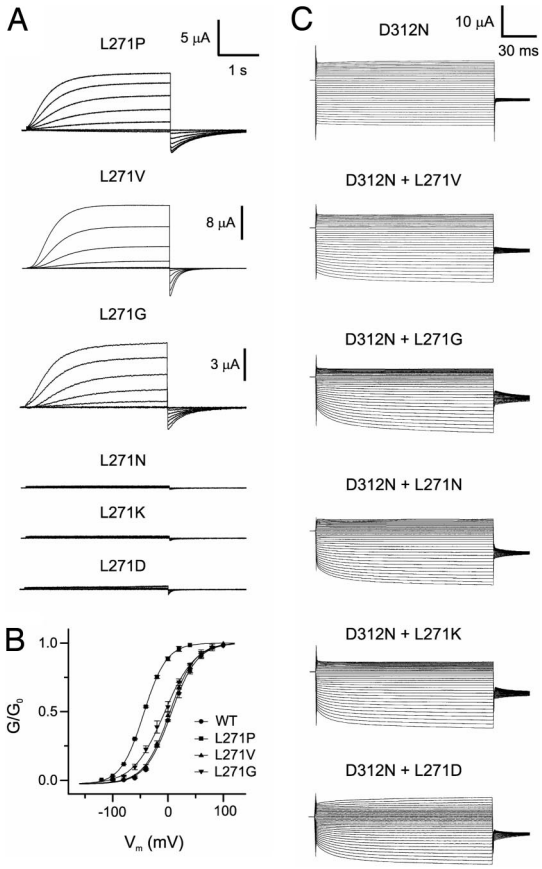

Fig. 3. Functional interaction of L271 and D312 in controlling voltage-sensing in the SKOR channel. (*A*) Whole-cell currents recorded from oocytes expressing SKOR mutants. The test voltages ranged from −120 to +100 mV in 10-mV increments. The bath solution contained 100 mM KCl. (*B*) Voltage-dependence of channel activation in the functional mutants, based on results in *A*, compared with wild-type SKOR. The voltage-dependence (*G–V*) was derived from currents and was fitted with Boltzmann equation $G/G_0 = 1/(1 + e^{-z_g \cdot F \cdot (V - V_{1/2})/RT})$, where z_g is the equivalent gating charge and $V_{1/2}$ is the half-activation voltage (20). (*C*) Whole-cell currents recorded from oocytes expressing SKOR mutants (D312N and various double mutants). The test voltages ranged from −200 to +120 mV in 10-mV increments, and the bath solution contained 100 mM KCl. The same scale bar is used for all recordings.

controlling voltage-dependent activation in SKOR. These results also demonstrate a dramatic phenomenon: that changes in only two amino acid residues can convert an outward-rectifying channel into an inward-rectifying channel.

When the available sequences of all plant Shaker-type K^+ channels were aligned [see supporting information (SI) Fig. 7], the corresponding residue of D312 in SKOR was conserved in another outward channel but was replaced by N in all of the inward channels. Together with the mutagenesis result, these findings suggest that the D312 position in SKOR must contribute significantly to the kinetic difference between SKOR and inward channels.

Our results from mutagenesis analysis suggest that voltage sensor (S4) alone is not the factor that specifies voltage-dependence in the inward or outward channels because the same S4 in the SKOR channel can sense either depolarized or hyperpolarized membrane potentials, depending on the specification of other domains, as shown with the SKOR mutants. This result demonstrates a crucial role for the sensor gate coupling, as Prole and Yellen (22) reported in the spHCN channel. They provided evidence, using cross-linking experiments, to support similar assertions. Their results showed that the S4–S5 linker and the C linker of spHCN physically interact (22). In other words, the S4 voltage sensor can sense membrane voltages, but S4 cannot determine the effect on the opening or closing of a

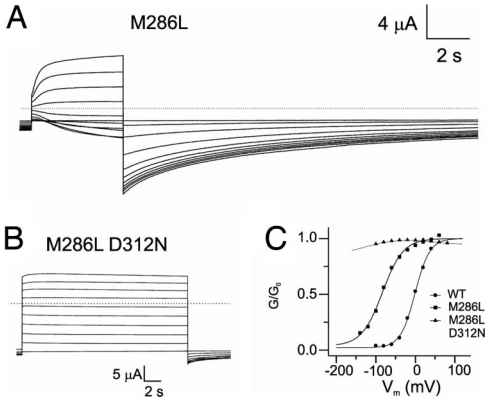

Fig. 4. Voltage-dependence is altered by M286L mutation. (*A*) Whole-cell currents of mutant M286L elicited by a voltage protocol to produce slow deactivation of large ''tail'' currents. Clamp potentials ranged from −150 to +50 mV with a 20-mV step. The current was elicited by using 20-s voltage pulses. The bath solution contained 100 mM K^+. The dotted line is a trace of current at reversal potential. (*B*) Whole-cell currents of double mutant (M286L/D312N) elicited by a voltage protocol from −100 to +100 mV with 20-mV increments. The dotted line is a trace of current at reversal potential. (*C*) The instantaneous currents in *A* and *B* and Fig. 1*B Left* were normalized to the largest current amplitude, to acquire the relative conductance (G/G_0) and then vs. the membrane potentials, using the equation described in Fig. 3.

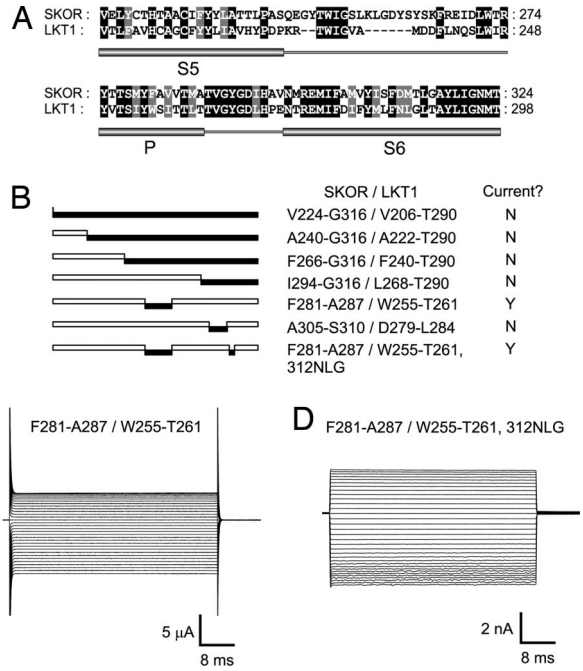

Fig. 5. Activities of hybrid channels generated by domain-swapping between SKOR and LKT1. (*A*) Alignment of the S5–P–S6 region of SKOR and LKT1, showing high homology between the two. (*B*) Diagrams showing the various swapping constructs. Portions of the LKT1 sequence (filled bars) were used to replace portions of the SKOR sequence (open bars). For example, the full-length filled bar indicates that the complete S5–P–S6 region of SKOR was replaced by the equivalent LKT1 region. (*C*) Whole-cell currents recorded from oocytes expressing functional hybrid channel (F281-A287/W255-T261) with clamp voltages from −200 to +120 mV in 10-mV increments. The bath solution contained 100 mM KCl. (*D*) Current traces recorded from a giant patch containing the functional hybrid channel (F281-A287/W255-T261) with additional mutation (312NLG), using the same voltage protocol as in SI Fig. 8.

particular channel unless specific interactions take place among a number of domains in between the sensor and the gate.

Besides the D312N mutation that occurred in 12 of the 30 mutants identified, other mutants that complemented CY162 contained single amino acid changes in other regions. In particular, a mutation in M286 (M-to-L) showed dramatic changes in electrophysiological properties compared with the wild-type SKOR. As shown in Fig. 4*A*, the mutant channel is activated by membrane potentials more positive than −140 mV, drastically shifting the potential to the more negative side, compared with the wild-type SKOR that is activated by membrane potentials more positive than −30 mV. In essence, the activating voltage range of M286L overlapped significantly with that of the inward channels (activated by potentials more negative than −100 mV). The extremely slow deactivation of this mutant channel led to a large tail current. The drastic change in the activation kinetics of the M286L mutant suggests that the residue at position 286 in SKOR also is critical for the voltage-sensing property. The M-to-L change in this SKOR mutant is interesting because the corresponding residue in the inward channels is L.

The M286 located in the pore α-helix is predicted to be close to D312 in S6, which was shown earlier to be critical for voltage-sensing. We speculated that these two positions may work cooperatively in voltage-dependent gating. We tested this idea by generating double mutants in both positions. The mutant channel containing D312N/M286L mutations showed kinetic properties similar to D312N alone (Fig. 4*B*), suggesting that the D312 residue is dominant and located further downstream along the voltage-dependent gating process. Fig. 4*C* shows the *I–V* curve of these mutants.

Because D312 plays an important role in keeping the SKOR channel outwardly rectified, we compared that domain with the equivalent domains in the inward channels. We found that three successive residues (D312, M313, and T314) in SKOR are changed into N, L, and G, respectively, in the inward channels. We mutated the DMT in SKOR into NLG, generating the mutant referred to as SKOR 312NLG. This mutant, like the D312N single mutant, lost voltage-dependence (SI Fig. 8*A*), which is consistent with previous studies (20, 21). No significant delay in activation kinetics was observed. In addition, this mutant conducted much larger current than wild-type SKOR or other mutants. These properties suggest that the voltage-gating pathway in this channel is disrupted and that the channel gate mostly stays in the open state. Because these residues are located in the center of S6, we speculate that they may constitute the channel gate or a critical link between the gate and the voltage sensor.

We also tested whether positions critical for voltage-sensing, including L271 and M286, may cooperate with 312NLG in S6. We made double mutants between SKOR 312NLG and L271P or M286L. Again, these double mutants essentially lost voltage-dependence (SI Fig. 8 *B* and *C*), which is similar to the property of the 312NLG mutant. Interestingly, SKOR 312NLG/L271P showed less current at membrane depolarization, and SKOR 312NLG/M286L conducted less current at membrane hyperpolarization (SI Fig. 8*D*). This result indicated that 312DMT in SKOR plays a dominant role in determining gating properties. However, changes in the double mutants implicated interaction of DMT with other sites, including L271 and M286.

Domain-Swapping Combined with Random Mutagenesis Confirms Domain Interactions in Voltage-Sensing. Along with the random mutagenesis approach, we used a domain-swapping procedure to determine domain contributions in channel-activation kinetics. We used LKT1 as an inward-rectified channel to replace the pore region (S5–P–S6) of outward-channel SKOR. Fig. 5*A* shows the alignment of this region between SKOR and LKT1. The most similar segment in the region is the distal half (C-end) of the S6 domain, consistent with the hypothesis that this domain forms the channel gate. A number of swapping mutants were made, as

described in Fig. 5*B*. Unexpectedly, most of these mutants were not functional channels. Only the swapping of the second half of the P domain (seven residues) resulted in a functional channel that again lost voltage-dependence (Fig. 5*C*). The 312NLG mutations, in combination with the swapping, did not change the current properties further, suggesting that the pore and gate domains are both required for voltage-dependent gating (Fig. 5*D*).

Among all swapping mutants, the most unexpected result was from the mutant in which the whole S5–P–S6 was swapped. We refer to this channel as SLV (SKOR protein with positions V224-G316 replaced by LKT1 V206-T290). This mutant gives a nonfunctional channel. At least one study has shown that the S5–P–S6 region formed an independent channel pore because the swapping of this region of the Shaker channel with the M1–P–M2 region of bacteria KcsA channel resulted in a fully functional channel with voltage-dependence (23). The negative result in our case suggested that regions in addition to the pore region also might be involved in the coupling process. To test this idea, we performed random mutagenesis on the hybrid channel SLV by using the method described in Fig. 1. We speculated that this nonfunctional channel might be caused by incompatibility of the hybrid domains and that random mutagenesis could result in subtle changes sufficient to recover the functionality. We conducted the random mutagenesis on SLV and screened for functional mutants according to the strategy described in Fig. 1. We recovered several mutants of the hybrid channel that complemented the yeast mutant and analyzed the mutant channels in the oocyte. As shown in Fig. 6*A*, a single mutation of T225A in the S5 domain (of the LKT1 protein) rendered the hybrid channel functional, but the channel showed little voltage-dependence. Because the corresponding residue in SKOR channel is E, we mutated T225 into E to determine the role of this residue in interactions with other regions. The hybrid SLV with T225E also is a functional channel without voltage-dependence (Fig. 6*B*). Interestingly, another random mutant with double mutations at T225A and V229A converted SLV into a functional channel with inward rectification. As shown in Fig. 6*C*, SLV T225A/V229A, like the LKT1 channel, shows delayed activation properties and opened upon membrane hyperpolarization, although the activation kinetics were not the same as with LKT1 (Figs. 1*B* and 6*D*). Because the pore region of the hybrid channel was from LKT1, it may not be surprising that single amino acid mutations changed the nonfunctional channel into an LKT1-like channel. However, this result is significant because it demonstrates a functional interaction between the pore region and the rest of the channel protein.

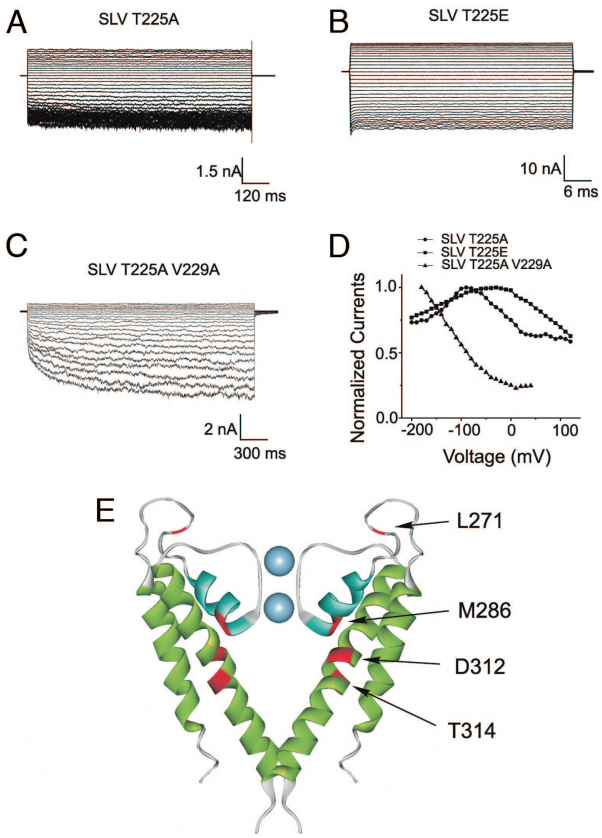

Fig. 6. Random mutagenesis rescued the nonfunctional channel SLV-SKOR. (*A–C*) Current traces were recorded from a giant patch containing SLV-SKOR with additional mutations, including T225A (*A*), T225E (*B*), and T225A plus V229A (*C*), by the same voltage protocol as in Fig. 5. (*D*) The currents were normalized to the largest current of SLV T225A/V229A to acquire the relative current (I/I_{max}) vs. membrane potentials. (*E*) Sites of several important residues for voltage-sensing and coupling are indicated in the model derived from the crystal structure of bacterial KcsA (4).

Concluding Remarks

The opening and closing of voltage-gated channels are controlled by membrane potential. There are several factors that function in the voltage-gating process. First, a voltage sensor is necessary to detect a change in the membrane voltage. It is widely accepted that the S4 transmembrane domain in the Shaker-type K^+ channels serves as the voltage sensor (18, 24). Second, there needs to be a gate structure that operates the opening and closing of the channel upon receiving a signal from the voltage sensor. Third, the sensor and the gate must be coupled so that the voltage signal can be translated into gating activities. Among these factors, what determines the voltage-sensing properties of a particular channel? Our results provide the following important insights into this question: (*i*) the voltage sensor (S4) alone does not distinguish the voltage-sensing range of inward or outward rectifiers because S4 in the outward-rectifying wild-type SKOR and inward-rectifying mutant SKOR was exactly the same, (*ii*) the physical gate located in the C-terminal half of the S6 helix is highly conserved and may not determine the voltage-sensing property or current rectification, and (*iii*) the potential interaction of several domains between the S4 sensor and the S6 gate is crucial for specifying the voltage-sensing range of a channel. This conclusion is supported by several findings. A striking example is that the D312N mutation in SKOR completely knocked out the voltage-dependence of the channel, whereas a combination of D312N with L271P converted outwardly rectifying SKOR into an inward rectifier. Furthermore, double mutations at T225A and V229A converted a dead hybrid channel into a functional channel with inward rectification. In this study, we found that several domains contribute significantly to the voltage sensor–gate coupling and control the range of voltage by which a channel is activated. These domains include the middle section of S6, the pore region before the selection filter, and part of the S5 domain.

Our study also provides critical clues for understanding the evolution of Shaker-type channels. The fact that an outward channel has "evolved" into an inward channel by simple single amino acid mutations suggests that channels with opposite voltage-sensing properties may have been derived from single mutations, instead of domain or exon shuffling, and, furthermore, that Shaker-type channels in plants may have the same ancestor.

Materials and Methods

Molecular Cloning Procedures. The *Arabidopsis KAT1* gene was cloned as described in ref. 19. *SKOR* was amplified by PCR, using a total-tissue cDNA library as template, and cloned into oocyte expression vector pGEMHE (25)

and pJR1136 yeast vector (18). *SKOR* is deposited in the GenBank database (accession no. NP_186934). Inserts in the constructed plasmids were fully sequenced, and clones identical to the defined sequences in GenBank were used for further characterization. The corresponding cRNA was transcribed *in vitro* by using the procedure described in ref. 19.

Random Mutagenesis and CY162 Complementation. Error-prone PCR was combined with DNA shuffling to randomly mutate the coding region of *SKOR*. Primers were used in a PCR under the conditions where *Taq* polymerase exhibits high error rates. Reactions were carried out in 100 μl in the presence of 0.2 mM each of dATP, dGTP, and dTTP; 3.4 mM dCTP; and 9 mM $MgCl_2$ or 0.15 mM $MnCl_2$. DNA shuffling was carried out according to Stemmer (16) and as modified by Lorimer and Pastan (17). DNA fragments from error-prone PCR containing the whole *SKOR* gene were digested into random fragments by the addition of 1 μl of DNase I (diluted to 0.2 ng/ml; Ambion) in the reaction buffer of 50 mM Tris·HCl and 10 mM $MnCl_2$ (pH 7.5) for 5 min on ice. The 50–200-bp fragments were purified by using the Qiaquick purification kit (Qiagen). To reassemble fragments, 20 μl of the spin column-purified DNA fragments were diluted into a 100-μl PCR mix containing 1$\times$ PCR buffer, 0.4 mM each dNTP, and 1 μl of *Taq* polymerase without primers. The reaction was conducted using the following program: 94°C for 5 min (94°C for 1 min; 45°C for 1 min; 72°C for 2 min) $\times$ 40 cycles; 72°C for 10 min. Five microliters of this reaction was used as template DNA in a 25-cycle PCR. The resulting fragments were digested with XbaI and HindIII and subcloned into pJR1136.

The randomly mutagenized *SKOR* sequences in the pJR1136 vector were transformed into yeast mutant CY162 that lacks high-affinity K^+ uptake systems and is unable to grow on the medium containing $<$1 mM K^+ (24). Transformed yeast cells were first grown on high-K^+ (50 mM) medium without uracil (ura$-$) to select all transformants. Cells from the surviving colonies were replated to ura$-$ medium containing 0.2 mM K^+, to select only those transformants that regained the capacity to grow on low-K^+ medium. The plasmids were isolated from the growing transformants and retransformed into yeast mutant CY162 to confirm the complementation. Independent SKOR mutant clones that complemented CY162 were sequenced to determine the sequence changes, compared with the wild-type SKOR. To confirm the mutations responsible for the altered property of the SKOR channel, the same mutations in the SKOR were regenerated by site-directed mutagenesis using a QuikChange protocol developed by Stratagene The newly generated mutants were tested again by using the yeast complementation system and subsequently in the oocyte system by voltage-clamp recording.

Electrophysiological Recording and Data Analysis. Oocyte expression and voltage-clamp recording were performed as described in ref. 19, with some modification. Unless otherwise indicated, the solutions used were as follows. The bath solution for two-electrode voltage clamp contained 10 mM KCl, 90 mM NaCl, 1 mM $CaCl_2$, 4 mM $MgCl_2$, and 10 mM Hepes (pH 7.4). For giant-patch recording, the bath solution contained 80 mM KCl, 20 mM NaCl, 4 mM $MgCl_2$, 2 mM EGTA, and 10 mM Hepes (pH 7.4). The pipette solution consisted of 5 mM KCl, 90 mM NaCl, 1 mM $CaCl_2$, 2 mM $MgCl_2$, and 10 mM Hepes (pH 7.4). For solutions with different K^+ concentrations, *N*-methyl-D-glucamine-Cl was used to maintain constant ionic strength. The single-channel current was recorded under the same conditions as the giant-patch recording. The voltage protocols used for patch-clamp recordings are described in the figure legends. All chemicals used in this study were purchased from Sigma–Aldrich.

Data analysis was performed by using Software Origin version 6.0 (OriginLab) to fit the *I–V* relationship and the *G–V* curve, as described by Liu *et al.* (26). All data are presented as mean $\pm$ SE (n = number of independent instances), and statistical analysis was performed using Student's t test.

ACKNOWLEDGMENTS. We thank Dr. E. Y. Isacoff (University of California, Berkeley, CA) for providing oocytes and B.B.B. for critical reading of the manuscript. This work was supported by National Science Foundation and U.S. Department of Agriculture grants (to S.L.) and National Natural Science Foundation of China Grant 30770177 (to L.L.).

1. Jan LY, Jan YN (1997) Cloned potassium channels from eukaryotes and prokaryotes. *Annu Rev Neurosci* 20:91–123.
2. Papazian DM, Schwarz TL, Tempel BL, Jan YN, Jan LY (1987) Cloning of genomic and complementary DNA from Shaker, a putative potassium channel gene from *Drosophila*. *Science* 237:749–753.
3. Kukuljan M, Labarca P, Latorre R (1995) Molecular determinants of ion conduction and inactivation in K^+ channels. *Am J Physiol* 268:C535–C556.
4. Liu YS, Sompornpisut P, Perozo E (2001) Structure of the KcsA channel intracellular gate in the open state. *Nat Struct Biol* 8:883–887.
5. Caprini M, *et al.* (2001) Structural compatibility between the putative voltage sensor of voltage-gated K^+ channels and the prokaryotic KcsA channel. *J Biol Chem* 276:21070–21706.
6. Shrivastava IH, Capener CE, Forrest LR, Sansom MS (2000) Structure and dynamics of K channel pore-lining helices: A comparative simulation study. *Biophys J* 78:79–92.
7. Lai HC, Grabe M, Jan YN, Jan LY (2005) The S4 voltage sensor packs against the pore domain in the KAT1 voltage-gated potassium channel. *Neuron* 47:395–406.
8. Grabe M, Lai HC, Jain M, Jan YN, Jan LY (2007) Structure prediction for the down state of a potassium channel voltage sensor. *Nature* 445:550–553.
9. Schroeder JI, Ward JM, Gassmann W (1994) Perspectives on the physiology and structure of inward-rectifying K^+ channels in higher plants: Biophysical implications for K^+ uptake. *Annu Rev Biophys Biomol Struct* 23:441–471.
10. Zimmermann S, Sentenac H (1999) Plant ion channels: From molecular structures to physiological functions. *Curr Opin Plant Biol* 2:477–482.
11. Schachtman DP, Schroeder JI, Lucas WJ, Anderson JA, Gaber RF (1992) Expression of an inward-rectifying potassium channel by the *Arabidopsis* KAT1 cDNA. *Science* 258:1654–1658.
12. Bei Q, Luan S (1998) Functional expression and characterization of a plant K^+ channel gene in a plant cell model. *Plant J* 13:857–865.
13. Gaymard F, *et al.* (1996) The baculovirus/insect cell system as an alternative to *Xenopus* oocytes. First characterization of the AKT1 K^+ channel from *Arabidopsis thaliana*. *J Biol Chem* 271:22863–22870.
14. Gaymard F, *et al.* (1998) Identification and disruption of a plant Shaker-like outward channel involved in K^+ release into the xylem sap. *Cell* 94:647–655.
15. Ache P, *et al.* (2000) GORK, a delayed outward rectifier expressed in guard cells of *Arabidopsis thaliana*, is a K(+)-selective K(+)-sensing ion channel. *FEBS Lett* 486:93–98.
16. Stemmer WP (1994) Rapid evolution of a protein *in vitro* by DNA shuffling. *Nature* 370:389–391.
17. Lorimer IA, Pastan I (1995) Random recombination of antibody single chain Fv sequences after fragmentation with DNaseI in the presence of Mn^{2+}. *Nucleic Acids Res* 23:3067–3068.
18. Whistler JL, Rine J (1997) Ras2 and Ras1 protein phosphorylation in *Saccharomyces cerevisiae*. *J Biol Chem* 272:18790–18800.
19. Liu K, Luan S (2001) Internal aluminum block of plant inward K(+) channels. *Plant Cell* 13:1453–1465.
20. Liu K, Li L, Luan S (2005) An essential function of phosphatidylinositol phosphates in activation of plant Shaker-type K^+ channels. *Plant J* 42:433–443.
21. Poree F, *et al.* (2005) Plant K(in) and K(out) channels: Approaching the trait of opposite rectification by analyzing more than 250 KAT1-SKOR chimeras. *Biochem Biophys Res Commun* 332:465–473.
22. Prole DL, Yellen G (2006) Reversal of HCN channel voltage dependence via bridging of the S4–S5 linker and Post-S6. *J Gen Physiol* 128:273–282.
23. Cao Y, Crawford NM, Schroeder JI (1995) Amino terminus and the first four membrane-spanning segments of the *Arabidopsis* K^+ channel KAT1 confer inward-rectification property of plant-animal chimeric channels. *J Biol Chem* 270:17697–17701.
24. Anderson JA, Huprikar SS, Kochian LV, Lucas WJ, Gaber RF (1992) Functional expression of a probable *Arabidopsis thaliana* potassium channel in *Saccharomyces cerevisiae*. *Proc Natl Acad Sci USA* 89:3736–3740.
25. Liman ER, Hess P, Weaver F, Koren G (1991) Voltage-sensing residues in the S4 region of a mammalian K^+ channel. *Nature* 353:752–756.
26. Liu K, Li L, Luan S (2006) Intracellular K^+ sensing of SKOR, a Shaker-type K^+ channel from *Arabidopsis*. *Plant J* 46:260–268.